Article ID: 1006-8775(2017) 01-0091-12

SENSITIVITY OF MESOSCALE CONVECTIVE SYSTEMS AND ASSOCIATED HEAVY RAINFALL TO SOIL MOISTURE OVER SOUTH CHINA

MENG Wei-guang (蒙伟光)[1,2], ZHANG Yan-xia (张艳霞)[1], LI Jiang-nan (李江南)[3],
DAI Guang-feng (戴光丰)[1], LI Hao-rui (李昊睿)[1], HUANG Yan-yan (黄燕燕)[1]
(1. Guangzhou Institute of Tropical and Marine Meteorology/Guangdong Provincial Key Laboratory of Regional Numerical Weather Prediction, CMA, Guangzhou 510080 China;
2. State Key Laboratory of Severe Weather, Chinese Academy of Meteorological Sciences, Beijing 100081 China;
3. School of Environmental Science and Engineering, Sun Yat-sen University, Guangzhou 510275 China)

Abstract: The impacts of soil moisture (SM) on heavy rainfall and the development of Mesoscale Convection Systems (MCSs) are investigated through 24-h numerical simulations of two heavy rainfall events that occurred respectively on 28 March 2009 (Case 1) and 6 May 2010 (Case 2) over southern China. The numerical simulations were carried out with WRF and its coupled Noah LSM (Land Surface Model). First, comparative experiments were driven by two different SM data sources from NCEP-FNL and NASA-GLDAS. Secondary, with the run driven by NASA-GLDAS data as a control one, a series of sensitivity tests with different degree of (20%, 60%) increase or decrease in the initial SM were performed to examine the impact of SM on the simulations. Comparative experiment results show that the 24-h simulated cumulative rainfall distributions are not substantially affected by the application of the two different SM data, while the precipitation intensity is changed to some extent. Forecast skill scores show that simulation with NASA-GLDAS SM data can lead to some improvement, especially in the heavy rain (≧50 mm) forecast, where there is up to 5% increase in the TS score. Sensitivity test analysis found that a predominantly positive feedback of SM on precipitation existed in these two heavy rain events but not with completely the same features. Organization of the heavy rainfall-producing MCS seems to have an impact on the feedback process between SM and precipitation. For Case 1, the MCS was poorly organized and occurred locally in late afternoon, and the increase of SM only caused a slight enhancement of precipitation. Drier soil was found to result in an apparent decrease of rainfall intensity, indicating that precipitation is more sensitive to SM reduction. For Case 2, as the heavy rain was caused by a well-organized MCS with sustained precipitation, the rainfall is more sensitive to SM increase, which brings more rainfall. Additionally, distinctive feedback effects were identified from different stages and different organization of MCS, with strong feedback between SM and precipitation mainly appearing in the early stages of the poorly organized MCS and during the late period of the well-organized MCS.

Key words: soil moisture; Southern China heavy rainfall; Mesoscale Convection System; numerical simulation
CLC number: P426.62 **Document code:** A
doi: 10.16555/j.1006-8775.2017.01.009

1 INTRODUCTION

Soil moisture (SM) is an important physical parameter of land-surface property. Its variations not only impact on the land-surface reflectivity, radiation, soil thermal capacity and vegetation conditions, but also affect the structure of the atmospheric circulation and variation of weather and climate through its effect on the redistribution of land surface energy and water. When SM anomalies take place, they usually last long and bring about "long-term memory" effect on a time scale that spans several months. Therefore, many of the previous work focused more on the effect of SM anomalies on successive general circulation and short-term climate change. As proved by a number of studies, the initialization of SM in numerical models is essential for climate simulation [1-3]. Is the SM also an important factor having impact on the short-term weather (such as convective rainfall)? It has been known and studied relatively little up to the present. Most of the existing work in this aspect focuses on some so-called "hot spots" where soil moisture may strongly affect rainfall, like the Sahara in Africa and southern part of the Rocky Plain in North America [4]. Due to its peculiar geographic conditions, the Sahara

Received 2014-12-06; **Revised** 2016-08-09; **Accepted** 2017-02-15
Foundation item: National Natural Science Foundation of China (40775068); Open Project for State Key Laboratory of Severe Weather, Chinese Academy of Meteorological Sciences (2009LASW-B03); Special Fund for Meteorological Scientific Research in the Public Interest (GYHY201106003, GYHY201406009)
Biography: MENG Wei-guang, Ph.D., Researcher, primarily undertaking research on Researcher, primarily undertaking research on tropical mesoscale meteorology and modeling.
Corresponding author: MENG Wei-guang, e-mail: wgmeng@grmc.gov.cn

exhibits not only significant seasonal changes in the land-surface water and heat flux, but also remarkable daily variations of the land-surface flux shortly after rainfall during monsoon or wet season, making the feedback of SM and precipitation outstanding. By means of observation and simulation, much work has been done on the effect of land-surface property such as vegetation cover and SM on the evolution of precipitation and convective systems over these areas[5-8], most highlighting the importance of SM distribution and variation on the precipitation. For the southern part of the Great Plain in North America, how convection evolves near the "dry line" attracted much attention. "Dry line" is a line of well-defined humidity contrast formed between the warm and humid air from the Gulf of Mexico and the dry and hot air from the western part of North America. The "dry line" has long been considered an area that is conducive to the initialization of convection. It has been observed that the difference in land-surface heat flux, which results from the difference in land-surface properties, may affect the development of the "dry line" and convection. For instance, studies found that the gradient of horizontal distribution of SM has great effect on the formation and shape of the "dry line" [9,10]). The distribution and variation of the SM can affect the thermal instability and then the initiation and development of convection by means of land-surface heat and moisture flux [11, 12]. Some modeling studies even found it possible for convection to either evolve vigorously or remain uninitialized near the "dry line" just by adding a small perturbation of moisture to a limited area in the low level around the dry line [13,14]. Summarizing what they studied, Chen et al. [15,16] pointed out that the location, intensity and coverage of simulated rainfall shows more sensitivity to the characterization and initial SM than applications with schemes of more detailed and real land-surface processes. Therefore, in addition to working in greater detail on the characterization of land-surface physical processes, it is also highly likely to improve model-predicted rainfall by refining the initialization of land surface features such as the SM.

Being one of the regions with complicated property of land surface, the southern part of China is subject to heavy rains during raining seasons that are of significant convection and closely related to the frequent activity of mesoscale convective systems (MCSs)[17-20]. What effect do the land-surface processes have on the formation of heavy rains? Is the evolution of heavy rain producing MCSs sensitive to the SM? They are both the issues worth studying. In this work, the WRF, a mesoscale modeling system, and its coupled model for land surface processes (Noah LSM) are used to run 24-h simulations of two typical heavy rain events in this part of China. The first one (Case 1) is a locally late-afternoon severe rain event that took place on March 28, 2009 in the Pearl River delta (PRD) region. The second one (Case 2) is a heavy rainfall event that took place in northern Guangdong within a better-defined frontal trough system. To study the possible effects of different initial SM conditions on the evolution of heavy rains and MCSs, two different SM datasets (one from NCEP-FNL and the other from NASA-GLDAS) are used to drive the models for comparison. Based on this, sensitivity experiments were carried out to investigate how the heavy rains and MCSs are sensitive to the variation of initial SM.

2 OVERVIEW OF THE TWO HEAVY RAIN EVENTS

Prior to the occurrence of severe rain in Case 1, the surface was in the control of a low pressure trough. The convective rain triggered localized frontogenesis, which has an important impact on the organized development of the heavy rain producing MCS. Fig. 1 presents the evolution of the convective system. It shows that a convective cloud cluster appeared firstly near Wuzhou in bordering areas between Guangxi and Guangdong province at around 06:00 UTC. Then, it moved downstream to the east and evolved into an MCS and brought thunderstorms, severe rain and hails to most part of western Guangdong and the PRD. Especially in the late afternoon, as the MCS moved close to Guangzhou (Fig.1c), a convective cloud cluster developed vigorously with a cloud-top temperature below -72℃, which was the main convective system that brought heavy rainfall to the city. For Guangzhou, the heavy rain took place mainly within 2 to 3 hours and by 13:00 UTC the convective system weakened and evolved into its dissipation stage.

Happening mainly in the northern part of Guangdong and impacting by the joint effect of cold air and southwesterly airflow, the rainfall amount in Case 2 was larger and covered a wider area. On the surface weather map, most of the southern China was dominated by a low-pressure trough at 00:00 UTC, the center of the low was located on the border between Guangxi and northern Vietnam, and a surface front within the eastward extending low-pressure trough was generally east-west oriented in the area north 25°N in northern Guangdong. As shown on the isotropic surface at 850 hPa, corresponding to the surface low, there was a low trough with cyclonic wind shear and southwesterly low-level jet stream to the south (figure omitted). It can be seen from the evolution of convective clouds given in Fig.2 that the heavy rainfall of Case 2 is also closely related to the activity of MCSs. The convection was initiated in the morning in northern Guangdong (Fig.2a) and developed into a large-scale cloud cluster after 03:00 UTC (Fig.2b, 2c and 2d). It was just the sustained effect of the MCS with such an extensive cloud cluster that brought abundant amount of rainfall to the region. In terms of organization, apparently, the MCS in Case 2 is better organized than that in Case 1.

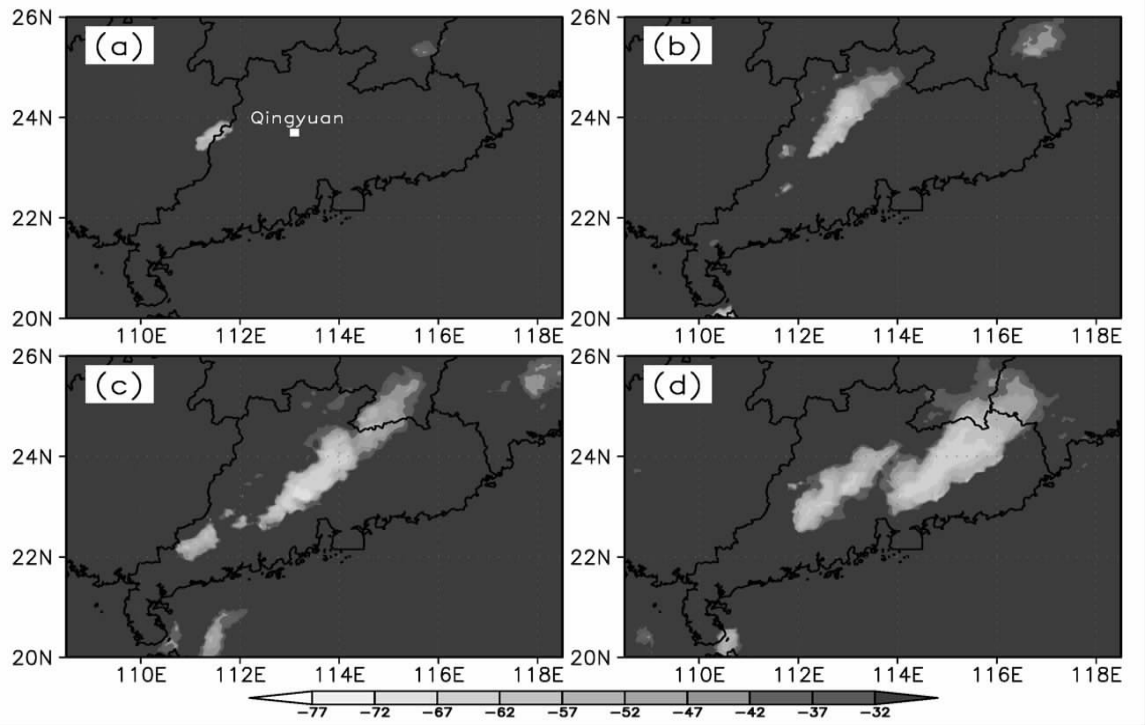

Figure 1. Cloud imagery of IR1 channel from satellite MASAT for March 28, 2009. (a): 06:00 UTC; (b): 08:00 UTC; (c): 10:00 UTC; (d): 12:00 UTC.

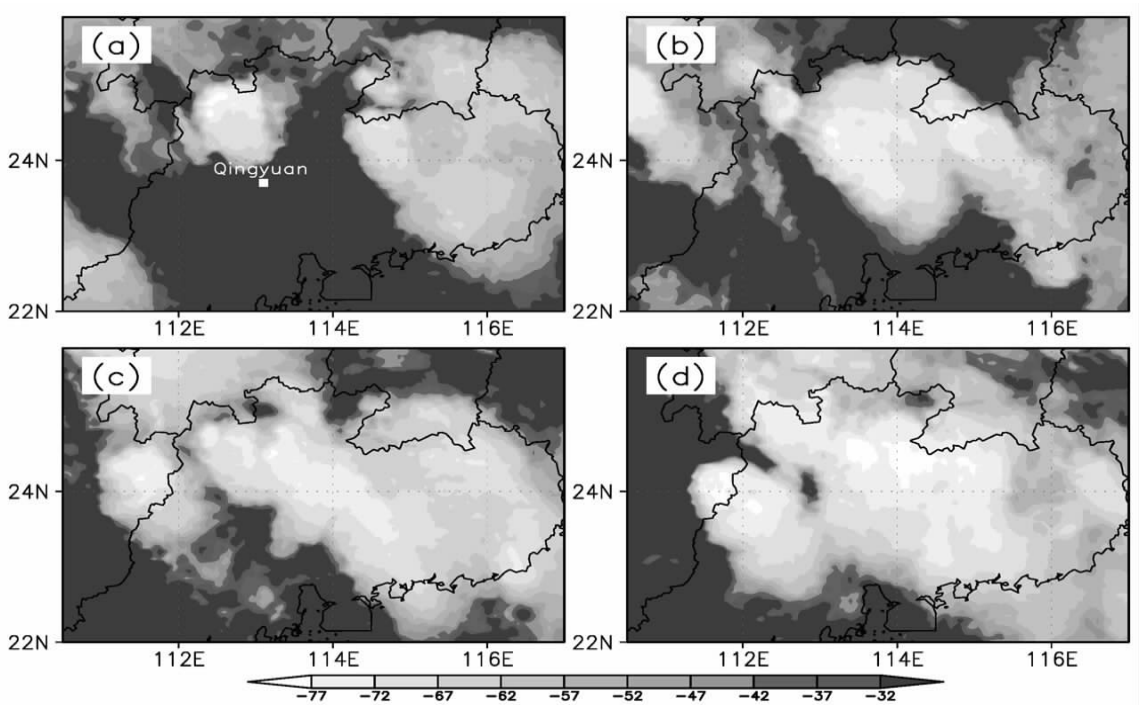

Figure 2. Same as Fig.1 but for May 6, 2010. (a): 01:00 UTC; (b): 03:00 UTC; (c): 05:00 UTC; (d): 07:00 UTC.

Figure 3 gives the distribution of 24-h accumulated rainfall of the two heavy rains. One can see that Case 2 brought larger amount of rainfall and coved wider areas compared to Case 1. The largest rainfall center in Case 2 recorded more than 400 mm and most of northern Guangdong received rainfall up to above 50 mm. Additionally, rainfall in Case 2 lasted longer than in Case 1. All these should be contributed by the fact that Case 2 occurred under an environment with a more distinctly large-scale controlling system. In contrast, the rainfall in Case 1 presented in a more localized area, with heavy rain mainly occurred around PRD and Guangzhou, and recorded only an accumulated rainfall of 140 mm in maximum.

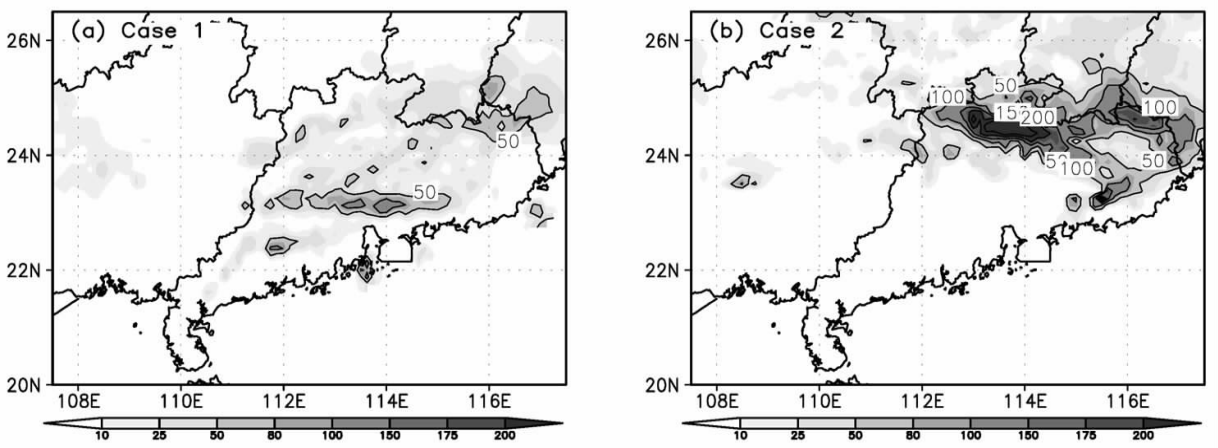

Figure 3. Distribution of 24-h accumulated rainfall of the two cases based on the observational analysis of automatic weather stations. Units: mm. (a): 00:00 UTC May 28 to 00:00 UTC May 29, 2009; (b): 12:00 UTC May 5 to 12:00 UTC May 6, 2010.

3 MODEL SETUP AND INITIALIZATION

3.1 *Model setup*

The WRFV3 [21] is used in the numerical studies. The model is run in two nested domains with grid points at horizontal resolutions of 12 km (D01) and 4 km (D02) respectively, and the outer domain D01 was centered on 113.0°E, 23.0°N. The two meshes take grid points of 263 × 189 and 301 × 202, respectively, and both have 35 layers in the vertical direction. The simulation is a one-way run. Our studies will focus on results from D02, so figures and tables listed below are mainly derived from the results of D02. In the simulation experiment, the following physical processes are used, namely, (1) the cloud physics scheme of Lin and the KF scheme for cumulus parameterization, (2) the RRTM longwave radiation scheme and Duhdia shortwave radiation scheme, and (3) the Monin-Obukhov surface-layer scheme, Noah land-surface scheme and YSU boundary layer scheme. Cumulus parameterization is used for the 4-km simulation because of the need for getting more real result. As shown by the preliminary experiments, the simulated distribution and rainfall amount of the two rainfall cases are closer to the observation if the cumulus parameterization scheme is used.

3.2 *Model initialization and experiment design*

The NCEP-FNL reanalysis is used as the initial and boundary-layer conditions of the model. To study the effects of the SM on the simulations, in addition to the NCEP-FNL SM data itself, another set of data from NASA-GLDAS (the Global Land Data Assimilation System) is used to drive the model for comparisons. At present, four non-online land-surface models (CLM, Mosaic, Noah and VIC) are used in the NASA-GLDAS. Large amount of observations are used to drive them to form a series of data describing land-surface conditions (including the SM, land-surface sensible heat flux and latent heat flux etc.). In this study, the SM data derived from the Noah-LSM were used, which has a 0.25° resolution[22].

First, the two different datasets are used as initial conditions to drive the model for comparison and to assess the effect of these two different SM data on the results. Then, based on the result from simulation with the NASA-GLDA data, or the control run, two groups of sensitivity experiments with variations on the initial SM were carried out to investigate the sensitivity of the simulations to the initial SM. Table 1 gives the designs for different experiments, in which EX-FNL and EX-GLD are the two comparison experiments, and the SM data from the NCEP-FNL and NASA-GLDAS were used respectively. The remaining are sensitivity experiments based on the control run with EX-GLD, in which the SM data on different soil layers are all decreased or increased by 20% and 60% relative to the normal values.

Table 1. Design of schemes for different experiments.

Scheme	Initial value of model SM	Variation of SM
EX-FNL	NCEP-FNL	Normal
EX-GLD	NOAA_GLDAS	Normal
EX-Dec60	NOAA_GLDAS	-60%
EX-Dec20	NOAA_GLDAS	-20%
EX-Inc20	NOAA_GLDAS	+20%
EX-Inc60	NOAA_GLDAS	+60%

As mentioned earlier, the Noah-LSM land-surface scheme was used in the simulation. In the WRF model, the Noah-LSM is a land-surface model with 4 soil layers respectively at the thickness of 10, 30, 60 and 100 cm. Since both the NCEP-FNL and NASA-GLDAS used the same LSM in their analysis systems, four layers of SM data from the two different sources are directly interpolated into the simulated domain in our experiments. Note that, as the NASA-GLDAS provided the SM data in the unit of kg/m^2, it needs to be converted to the unit of m^3/m^3 of SM data used in the

WRF model.

To cover the evolution processes of the two heavy rains, the model integration for Case 1 starts from 00:00 UTC May 28, 2009 while that of Case 2 from 12:00 UTC May 5, 2010, both for 24 h.

4 SIMULATION RESULTS AND ANALYSIS

4.1 *Comparison of two initial SM data*

In general, the value of SM from NASA-GLDAS is smaller than that of NCEP-FNL. With higher resolution, the former, which is derived by driving the land-surface model with large amount of observations, generally shows some more detailed structure of distribution. Here, only the distribution of the upper soil layer (0 to 10 cm) SM of D02 is given (Fig.4) at the time of 00:00 UTC May 28, 2009, when the model began integration in Case 1. Both SM datasets show that areas in western Guangxi is relatively dry but they differ much in other locations. For the NCEP-FNL, the SM is all above 0.32, especially for areas over most part of central Guangdong and northeastern Guangxi where it is usually greater than 0.36. While for the NASA-GLDAS, SM in areas connecting Guangdong and Guangxi and eastern Guangdong are relatively dry, with values being only 0.24 and much greater contrast between the dry and wet areas.

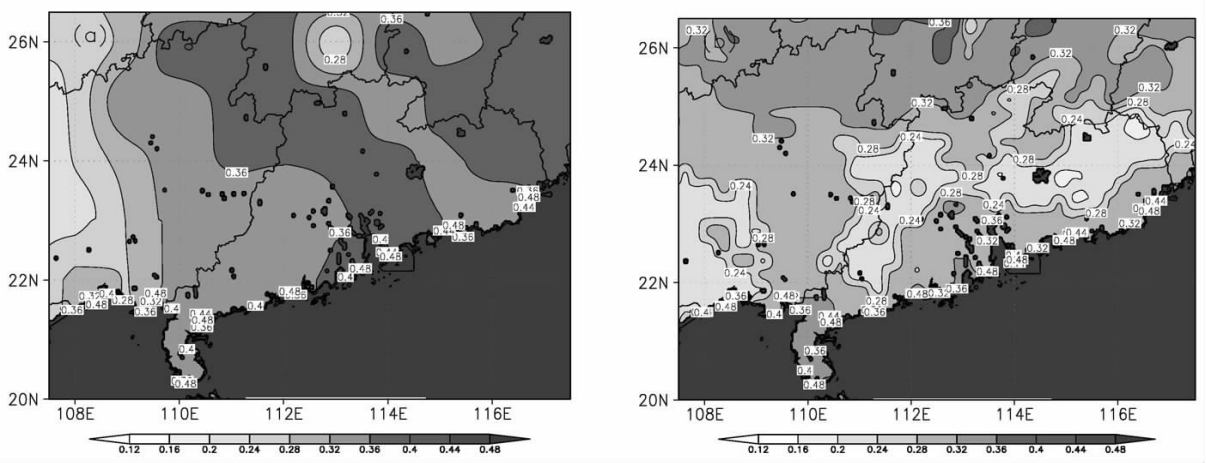

Figure 4. Distribution of initial SM at 00:00 UTC for May 28, 2009.

4.2 *Experiment of the comparison experiments*

Figures 5 and 6 give the distribution of 24-h accumulated rainfall for the two heavy rains simulated by different experiments. Generally, the application of the two different SM data only has a little effect on the rainfall simulation. Compared to the real rainfall (see Fig.3), though it shows that simulations of both rainfall cases are still different from the observation to some extent in rainfall amount and locations (Fig.5), they capture most features of the real one. For instance, for Case 1, though the two comparison experiments both simulated a wider area in the 50 mm rainfall, they are quite similar to the observation in the reproduction of the 100 mm rainfall areas and mainly concentrated around Guangzhou. Especially for EX-GLD, in which the simulated 50 mm rainfall area is a little bit larger than that of EXP-FNL while the 100 mm rainfall area are closer to Guangzhou. In terms of rainfall magnitude, the simulated rainfall in both experiments are larger than 160 mm within the main rainfall area (as indicated by the rectangular in the figure), about 20 mm larger than the observation (140 mm). For Case 2, though the simulated rainfall center located at the border areas between northeastern Guangdong and Fujian was more northward and eastward in location by the two experiments, the rainfall center in northern Guangdong is better simulated and similar to the observation. As shown in Fig.6, though EX-GLD resulted in a slightly larger area in the simulation of 100 mm rainfall over northern Guangdong than that of EX-FNL, the latter is more successful in simulating the intensity of rainfall. The simulated maximum rainfall center in EX-FNL reached 270 mm, while the former's has only a maximum rainfall of 220 mm, both smaller than the actual value of 400 mm.

To objectively evaluate the impacts of application of the two different SM data on the rainfall simulations, a contingency table was analyzed by using the observed and predicted rainfall over the entire domain D02. Following the quantities defined in Table 2, a number of statistical variables, including percentage of successful predictions (SUCC), percentage of successful predictions for rainfall episodes (SUCCT), percentage of successful predictions for non-rainfall episodes (SUCCNT), and percentage of correct prediction considering only rainfall episodes (TS) and fractional bias (FBIAS), are calculated. In formulas listed in the table, A is the number of correct rainfall predictions (rain predicted and observed), B the number of underestimated predictions (rain not predicted but observed), C the number of overestimated predictions (rain predicted but not observed) and D the number of correct 'non-rainfall' predictions (rain not predicted and not observed).

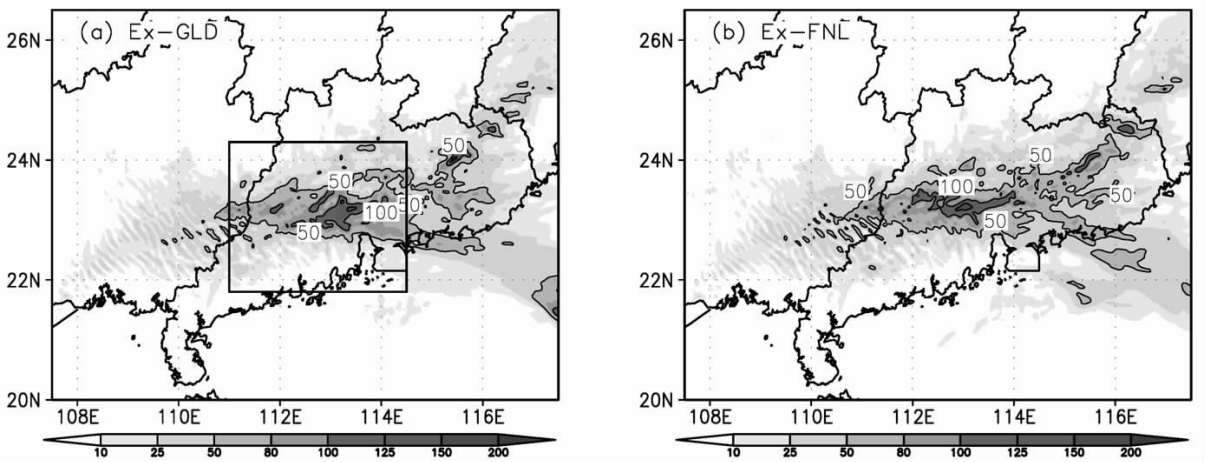

Figure 5. Distribution of 24-h accumulated rainfall simulated for Case 1 (from 00:00 UTC March 28 to 00:00 UTC March 29, 2009). (a): EX-GLD; (b): EX-FNL.

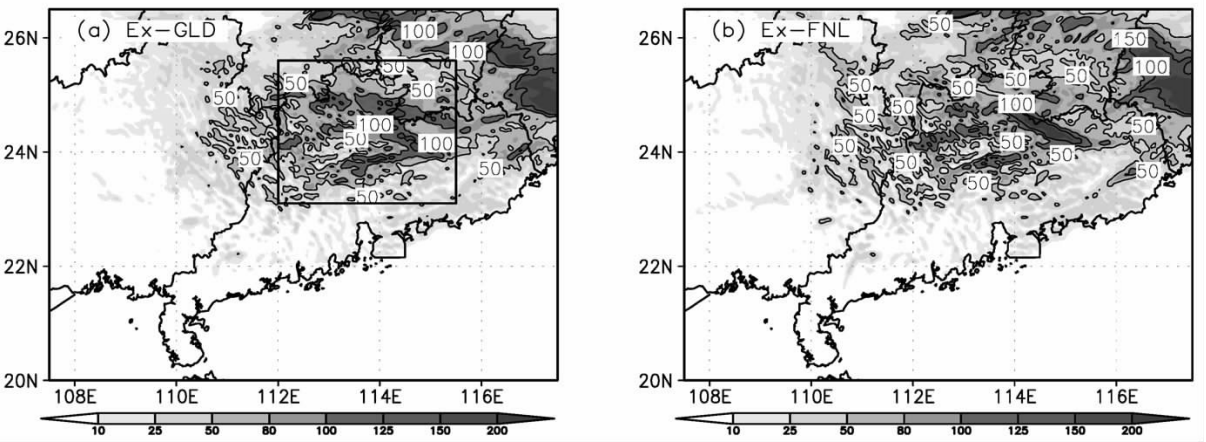

Figure 6. Same as Fig. 5 but for the time from 12:00 UTC May 5 to 12:00 UTC May 6, 2009.

Table 2. Formula determining the content of Tables 3 and 4.

Variable	Formula	Optimum score
SUCC	100×(A+D)/(A+B+C+D)	100
SUCCT	100×A/(A+B)	100
SUCCNT	100×D/(C+D)	100
TS	100×A/(A+B+C)	100
FBIAS	(A+C)/(A+B)	1

The observed rainfall data used for the calculation came from automatic weather stations located within D02 and the predicted rainfall was interpolated onto the observation sites before the calculation was carried out. Tables 3 and 4 listed different index calculated for precipitation thresholds of 0.1, 10, 25, 50, and 100 mm. The "difference" indicates the changes made to EX-GLD relative to EX-FNL and the values corresponding to an increase of the forecast skill are given in bold type.

Table 3 shows the assessment results for the two experiments for Case 1. EX-GLD is somewhat decreased rather than improved relative to EX-FNL in terms of SUCC and SUCCNT for different thresholds of rainfall. Nevertheless, the former improved much in SUCCT for rainfall of 50 and 100 mm, at 9.46% and 46.16%, respectively. This must be related to the fact mentioned above—area with simulated rainfall is larger than the observation, area of 50 mm rainfall predicted by EX-GLD is larger than that of EX-FNL in the PRD region and much concentrated in Guangzhou. By comparing their deviation (FBIAS), it is noted that the EX-GLD is indeed having larger FBIAS in thresholds of above the heavy rain (50 mm) intensity. It is also just because of it, especially because the predicted rainfall center is more similar to the observation and closer to Guangzhou, the number of underestimated predictions is reduced and that of SUCCT is increased. However, as the number of overestimated predictions increase, there was less improvement in TS, which just improved a little by just 0.88% and 4.49%, respectively for the precipitation thresholds of 50 mm and 100 mm.

Table 4 gives results for Case 2. The results of EX-GLD generally has somewhat improved for different precipitation thresholds. The SUCCT for the 50 mm rainfall forecast has risen by 3.9% and the SUCCT for 100 mm by 18.37%. As a result, the TS for

precipitation the thresholds of 50 mm and 100 mm increased 5.49% and 10.58% respectively. As a result, it can be concluded that although EX-FNL predicted more rain for Case 2, the EX-GLD seemed to have statistically better prediction effects. For both cases, FBIAS has greater values in EX-GLD, suggesting that EX-GLD generally over-predicts rainfall on the one hand, and the distribution of rainfall stations used for the assessment would also increase the FBIAS on the other. Modeling precipitation, usually presented as continuous distribution, may also contribute to the higher FBIAS.

Table 3. Summary of statistical indexes for Case 1 (the heavy rain on March 28, 2009).

Exp.	Rain range/mm	Accuracy (SUCC)	Hit (SUCCT)	Anti-hit (SUCCNT)	Threat score(TS)	Deviation (FBIAS)
EX-FNL	0.1	83.21	97.47	17.87	82.66	1.15
	10	64.91	84.50	52.13	48.73	1.58
	25	66.59	82.92	62.99	30.97	2.51
	50	79.56	78.38	79.67	24.17	3.03
	100	95.00	7.69	95.64	1.11	6.00
EX-GLD	0.1	83.27	96.58	22.26	82.57	1.14
	10	62.83	82.08	50.57	46.57	1.58
	25	65.64	77.33	63.06	28.92	2.45
	50	78.16	87.84	77.28	25.05	3.39
	100	93.37	53.85	93.67	5.60	9.15
difference	0.1	**0.06**	-0.89	**4.39**	-0.09	-0.01
	10	-2.08	-2.42	-1.56	-2.16	0.00
	25	-0.95	-5.59	**0.07**	-2.05	-0.06
	50	-1.40	**9.46**	-2.39	**0.88**	**0.36**
	100	-1.63	**46.16**	-1.97	**4.49**	**3.15**

Table 4. Summary of statistical indexes for Case 1 (the heavy rain on May 6, 2010).

Exp.	Rain range/mm	Accuracy (SUCC)	Hit (SUCCT)	Anti-hit (SUCCNT)	Threat score(TS)	Deviation (FBIAS)
EX-FNL	0.1	87.17	100.00	0.00	87.17	1.15
	10	60.11	98.31	8.22	58.67	1.66
	25	55.09	92.86	26.65	47.04	1.90
	50	64.44	75.88	60.04	37.19	1.80
	100	81.45	21.43	90.95	13.64	0.79
EX-GLD	0.1	87.17	100.00	0.00	87.17	1.15
	10	59.69	98.79	6.58	58.54	1.68
	25	56.21	94.81	27.14	48.18	1.92
	50	68.34	84.92	61.97	42.68	1.84
	100	82.98	39.80	89.82	24.22	1.04
difference	0.1	0.00	0.00	0.00	0.00	0.00
	10	-0.42	**0.48**	-1.64	-0.13	**0.02**
	25	**1.12**	**1.95**	**0.49**	**1.14**	**0.02**
	50	**3.90**	**9.04**	**1.93**	**5.49**	**0.04**
	100	**1.53**	**18.37**	-1.13	**10.58**	**0.25**

4.3 *Results of sensitivity experiment*

4.3.1 EFFECT OF SM ON REGIONAL MEAN RAIN RATE

It is known from the analysis above that the application of NASA-GLDAS SM data has somewhat improved the simulation of the two cases of heavy rain, more obviously shown in the TS score. However, is it necessarily connected with the characteristic presence of the NASA-GLDAS SM data? It is difficult to understand more about it because the quality of these data is hard to assess due to the scarcity of observed SM, and the difference in simulated rainfall is not large enough to explain from the prospective of either upper-level circulation patterns or meteorological conditions (such as water vapor and instability) difference at the near-surface layer).

Nevertheless, by means of sensitivity experiments with variation of initial SM, we can understand the problems from a different prospective. In the followings, EX-GLD is taken as a control run to study the result achieved by rerunning the model after the initial SM is varied by different degree. As shown in section 3.2, the sensitivity experiment is conducted by increasing 20% and 60% and decreasing 20% and 60% of the initial SM respectively (see Table 1).

It is also shown in the sensitivity experiment that such variations of the initial SM neither alter the

generation of heavy rain nor have considerable effect on the distribution pattern of the rainfall (figure omitted). Here, by means of considering the variation of area mean rainfall amount for different experiment, we try to understand the effect of varying SM on precipitation. The mean areas taken are referred to the rectangular domains in Figs. 5a and 6a, which cover the main areas of heavy rain in Cases 1 and 2.

Figure 7 gives temporal variation of the area mean rain rates of different experiments. Fig. 7a shows that the rain in Case 1 takes place mainly from midday through sunset, which is consistent with the convection actually observed. In general, there is positive feedback between the rainfalls in Case 1 and the SM, though the increase in the initial SM can only result in slight increase in the rain rate while the decrease can bring about significant decrease in it. As shown in the computation, the increase is only 3% while the decrease is more than 20%, reflecting that the rainfall of Case 1 is more sensitive to the reduction of SM. The figure also shows that the sensitivity of rain rates to SM is mainly presented at the initial development stage of the MCS that brings the heavy rain. When the MCS evolved into its late life cycle, such response of rain to the SM variation becomes weaker or even shows some reversed characteristics.

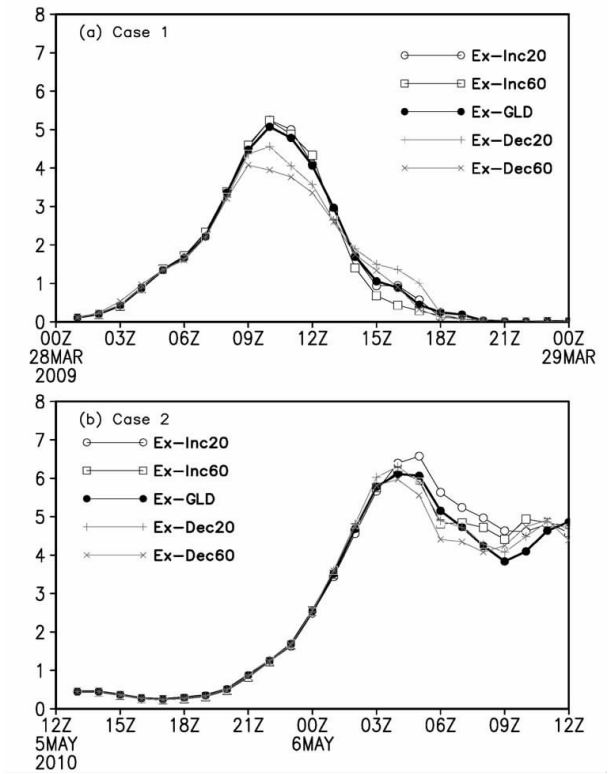

Figure 7. Temporal evolution of the area mean rain rates in Case 1 (a) and Case 2 (b). Units: mm/h.

The positive feedback also presents in Case 2, but with features not entirely the same as that is revealed in Case 1. Case 2 is more sensitive to the increase of the initial SM, which can lead to evident increase of rain rate. As shown in Fig.7b, rainfall in Case 2 begins in the morning and lasts until the evening, which can be considered as a continuous rainfall process. The largest change in rain rate due to initial SM increase mainly occurred at late afternoon and early evening. For instance, the largest enhancement in EX-Inc20 occurs at 09:00 UTC, while that of EX-Inc60 happens at 10:00 UTC, both over 20% as compared to the control run. In contrast, rainfall is less sensitive to the reduction of the initial SM and for EX-Dec20, the rain rate in most times presents as increases rather than decreases compared to the control run. Only when the initial SM decreases by relatively large amount will the rain rate reduce significantly. Additionally, although the obvious rain rate changes in the two cases both mainly occur from midday to sunset, one can note that the heavy rain producing MCS in Case 2 is now at its late life cycle compared to MCS in Cases 1, suggesting that at different stages, rainfall changes of convective system in the two rainfall cases respond differently to the SM variation.

4.3.2 EFFECT OF SM ON THE AREA INTEGRATION RAINFALL

By analyzing changes in the area integration rainfall during different rainfall stages, we can better understand this difference. Fig.8 gives the variation of the area integration rainfall for different sensitivity experiments at different time period by comparing it to the control run. Following the evolution features of MCSs and rainfall in the two cases, the figure gives these values in the second and third 6-h periods for Case 1, and in the third and fourth 6-h periods for Case 2 during the entire 24-h integration time. The two consecutive 6-h periods are roughly corresponding to the early (late) development stage of the MCS brings heavy rain with Case 1 (Case 2). The figure also presents changes over the entire 24-h integration. Fig. 8a clearly shows that the rainfall of Case 1 is more sensitive to the reduction of SM, which mainly occurred in the second 6-h period or at the early development stage of the MCS, with reduction of SM by 20% and 60% possibly resulting in rainfall decrease by 54×103 mm and 92×103 mm respectively, while the increase of SM by the same amounts only induces rainfall enhancement by 15 × 103 mm and 21 × 103 mm respectively. The figure also shows the reversed response of rainfall to SM during the late life cycle of MCS: the increased SM results in the decrease of rainfall, and small reduction in SM may lead to increase in rainfall instead.

Figure 8b also shows that increased SM results in the increase of rainfall during the late life cycle of MCS (the fourth 6-h period). It is, however, noted that with the increase of SM increment, the rainfall does not increase proportionally and even decreases in the early life cycle of MCS. Generally, rainfall in Case 2 is less sensitive to SM reduction than to SM increase. The fact that rainfall presents small variation as SM reduction

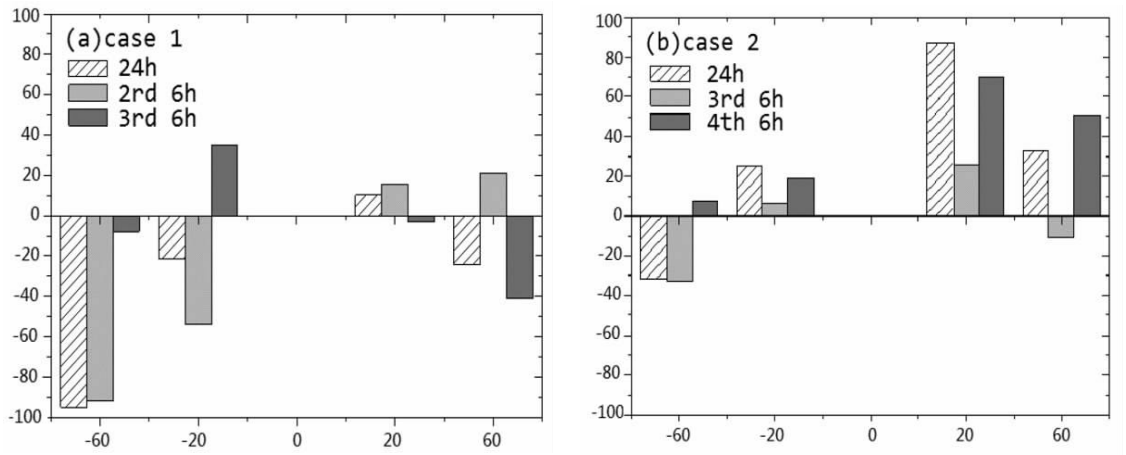

Figure 8. Variations of area integration rainfall between the sensitivity experiment and the control run. Units: mm. (a): Case 1; (b): Case 2. x-coordinate defines the percentage variation of SM relative to the control run (Units; %) and y-coordinate defines the variation of area integrated rainfall relative to the control run (Units: 10^{-3}mm).

increases and mild reduction of SM results in rain rate increases rather than decreases can be evidence supporting the above conclusion.

4.3.3 EFFECT OF SM ON THE PROPERTY OF ATMOSPHERIC CONVECTION

Why does the feedback between rainfall and SM in the two heavy rain cases show differently? It can be better understood by studying land-atmosphere process variations induced by SM changes and their effect on atmospheric convection property. Figs.9 and 10 give the temporal evolution of area mean land-surface flux, convective available potential energy (CAPE) and boundary layer height for the two cases of heavy rain. For simplicity, the figure gives only the curves of variations of the control run and the experiments with the 20% SM increasing and decreasing.

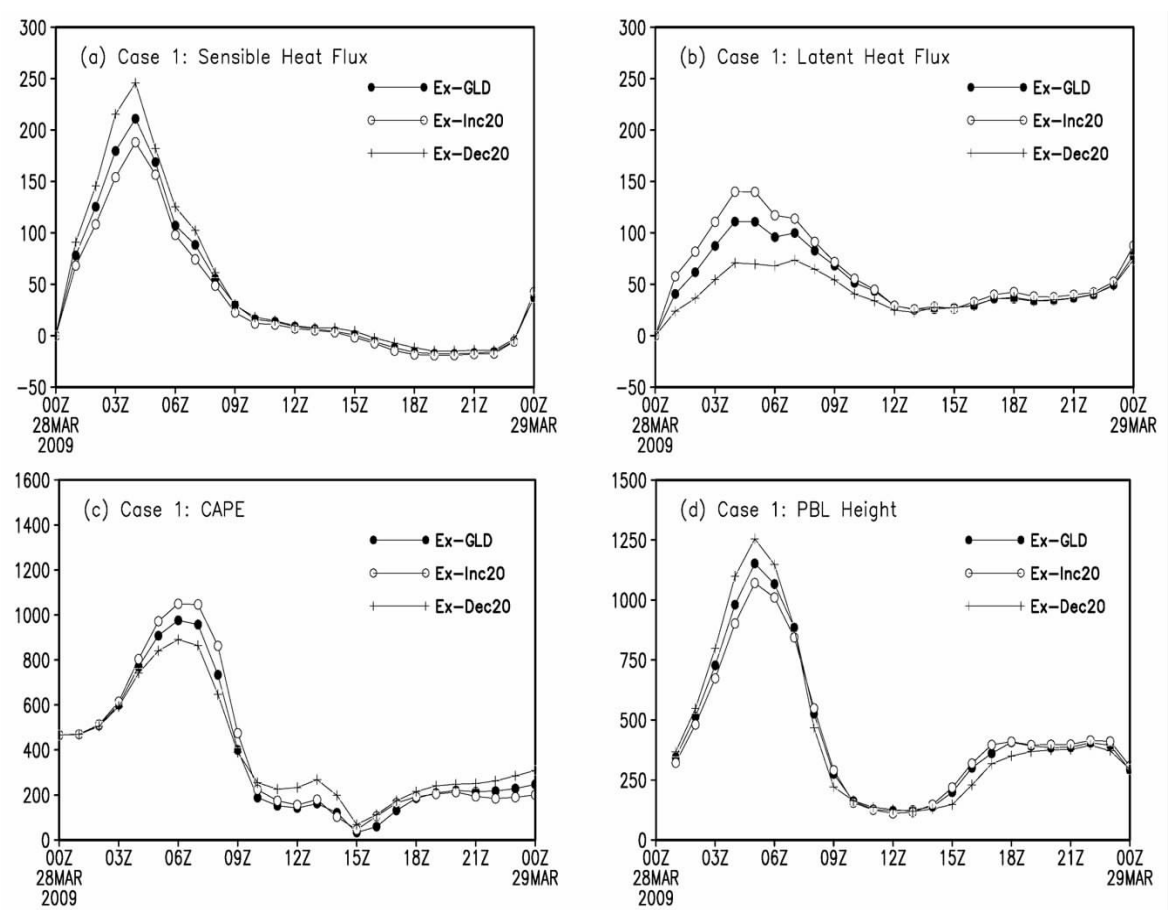

Figure 9. Temporal evolution of area mean land-surface sensible heat flux (a, units: W/m^2), latent heat flux (b, units: W/m^2), CAPE (c, units: J/kg) and height of the boundary layer (PBLH, d, units: m) for Case 1.

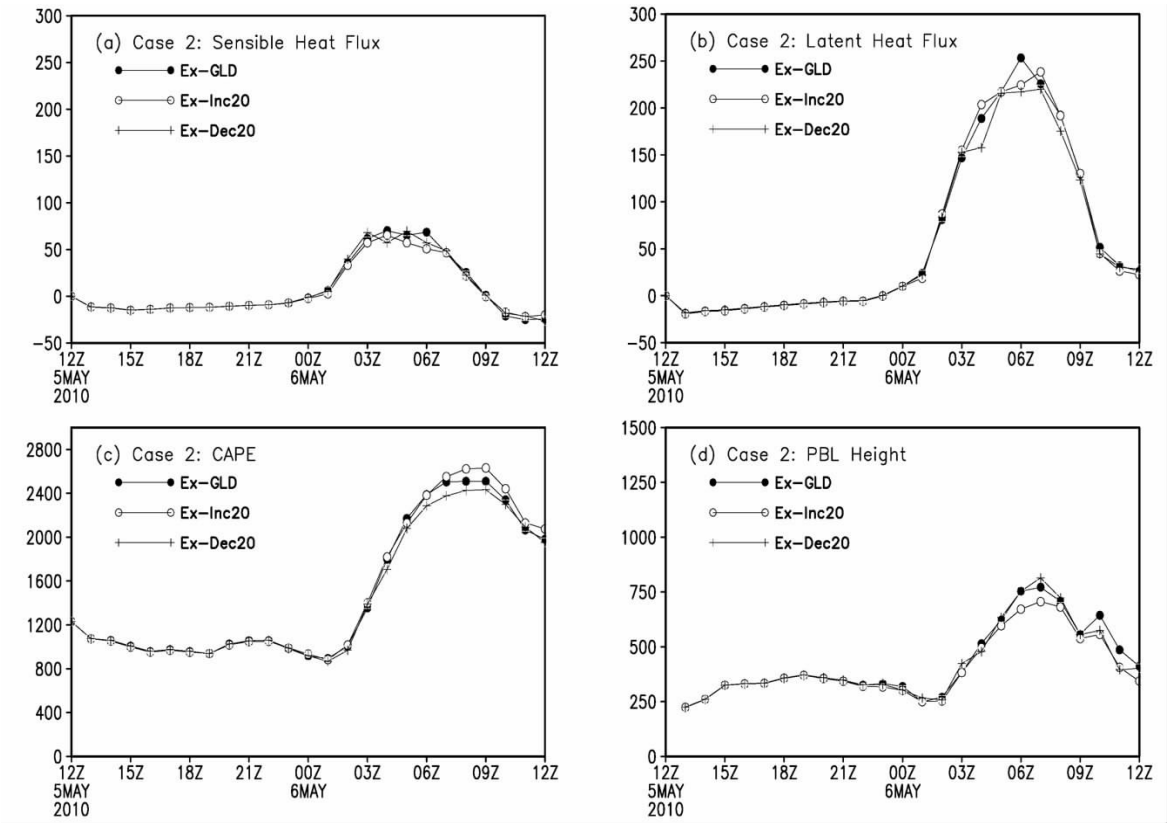

Figure 10. Same as Fig. 9 but for Case 2.

Due to the differences in the time and environment for which the MCSs initiated and evolved in the two cases of heavy rain, especially in the coverage of cloud clusters and the form of organization and development (Figs.1 & 2), the land-surface fluxes and their variations are affected. For Case 1, the convective cloud system begins after midday in a small area. As the diurnal solar radiation is not much blocked by clouds, the maximum of land-surface sensible heat flux can be more than 200 W/m^2 with Case 1 but less than 100 W/m^2 with Case 2. As shown in the result, the land-surface latent heat flux is larger than that of Case 1. For the same reason, the land-surface flux in Case 1 responses much sensitively to the change of SM than that of Case 2. Take the midday time when the flux is largest for instance, for the 20% increase (decrease) of SM in Case 1, the sensible heat flux can be reduced (enhanced) by 10% to 15% and the latent heat flux by 25% to 35%, while such a response is less sensitive in Case 2.

The variation of land-surface flux by impacting on the low-level atmospheric property could have a significant effect on the atmospheric convective property. Figs. 9 and 10 show that the environmental atmospheric CAPE values grow significantly during midday and reach their maximum afternoon. Although the CAPE value in Case 1 is less than that in Case 2, the former is only around 1,000 J/kg at maximum while the latter can be greater than 2,000 J/kg in most of the daytime. Because of the higher sensitivity of land-surface flux to the SM, the variation of CAPE due to the SM change is more significant in Case 1.

By analyzing the changes of θ_e (pseudo-equivalent potential temperature) and θ_{se} (saturated pseudo-equivalent potential temperature), two important atmospheric parameters, the sensitivity of CAPE to the variation of the land-surface flux can be accounted for. Fig.11a presents the vertical profiles of θ, θ_e, and θ_{se} regionally averaged at 06:00 (after midday) for the control run in Case 1, which shows the atmospheric conditions at the early life cycle of the convective system. With the increase of height, θ_{se} decreases at low levels of the atmosphere, demonstrating that the environmental atmosphere at low level is in conditional instability; as long as an air parcel is lifted from the surface to the level of free convection (LFC), its potential unstable energy will be released to trigger convection. Following the method of Holton[23], the height of the LFC can be estimated. As θ_{se} conserves during the uplifting of the air parcel, the latter will follow the vertical dashed curve as shown in Fig.11a. By comparing this curve with the vertical profile of the ambient atmosphere (θ_{se}), the buoyancy of the air parcel can be detected and its potential LFC can also be determined. In the figure, the point at which the vertical dashed curve intersects with the profile at the low level indicates where the potential LFC is while the point they meet at the upper level suggests the height of a level of neutral buoyancy (LNB). Here in this work,

"potential" means that it must be possible for the air parcel to get saturated and overcome negative buoyancy to be lifted to LFC. Generally speaking, if LFC is below the height of the boundary layer, the vertical mixing inside the boundary layer alone—triggered by thermal turbulence—is able to lift the surface air parcel to LFC and cause convection. The height of intersection in this figure is about 1,100 m, which is not much different from the average height of the boundary layer as indicated in Fig.9d. As a result, Case 1 being as a localized afternoon heavy rainfall event, the thermodynamics may be an important factor to initialize the convection. Of course, the large-scale background, such as the lifting mechanism arising from the convergence of surface troughs in this case, also has contribution to the convective initialization.

Figure 11b gives the profiles of θ_e and θ_{se} determined with the other two sensitivity experiments (EX-Inc20 and EX-Dec20) in Case 1. For clarity, the figure only presents what it looks like below the height of 5 km and does not plot the variation curve of the control run, which lies between the two experiments. Compared to the control run, EX-Inc20 and EX-Dec20 resulted respectively in a higher and a lower θ_e value on the surface, leading to the uplifting track of the air parcel with EX-Inc20 (the line CD in Fig.11b) being to the right of that of EX-Dec20 (the line AB in Fig.11b). Besides, EX-Inc20 may lead to an even lower θ_{se} in the boundary layer than that of EX-Dec20, contributing to a lower LFC in the former. As the value of CAPE is proportional to the height of LFC and LNB and the area of enclosure formed between them and θ_{se} (the area of slanted lines in Fig.11a), the area will vary substantially with the variations of uplifting track and LFC due to minute changes in low-level θ_e and θ_{se}. In Fig.11b, as the uplifting track in EX-Inc20 is to the right of that of EX-Dec20, it results in a larger value of CAPE. Besides, with a lowered LFC, convection in CASE 1 may be triggered more easily and develop more vigorously. For EX-Dec20, however, the reduced CAPE value and increased LFC would inhibit the development of convection. It can be concluded that it is just the changes of thermodynamics in the boundary layer caused by SM variations that results in the high sensitivity of rainfall simulation to the SM in the early stage of Case 1.

Comparatively speaking, as Case 2 is much affected by the large-scale background systems, the SM change can only result in a little change in the land-surface flux. In addition, as convection was initiated in the early morning, it has little effect on the initiation of convection and rainfall happened during this period. At the late development stage, however, as convection developed with more organization features, the convective rainfall appears to be more sensitive to the variation of CAPE. Rainfall in Case 2 increased much more significantly due to increased SM, which

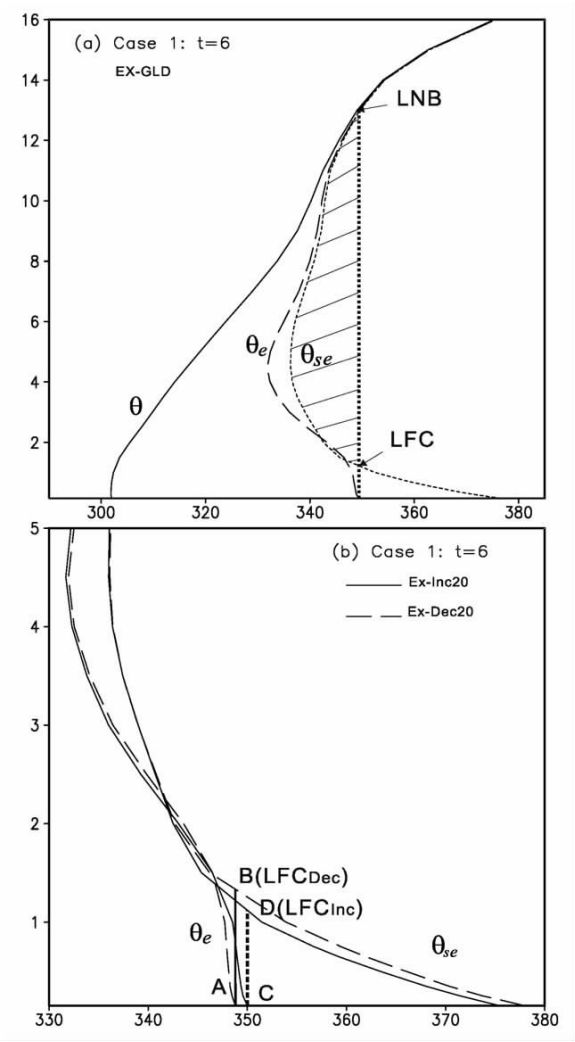

Figure 11. Area averaged vertical profiles of θ, θ_e and θ_{se} for the control run (a) and EX-Inc20 and EX-Dec20 (b) in Case 1. Units for the *y*-coordinates: km; units for the *x*-coordinates: K.

should be induced by wet soil with higher CAPE. It is shown in Fig. 10c that as compared to the other elements, the CAPE value varies more regularly because of the change in SM; it gets larger with increased SM and becomes smaller when the SM decreases. This conclusion is similar to previous results, like Gantner et al.[24]. In their study on the effect of SM in West Africa on the evolution of MCSs, they found that the feedback between precipitation and soil moisture is linked with the developmental stage of a convective system; during the mature stage in which convection is more organized, rainfall usually has positive feedback with the SM and environmental atmosphere with wet soil has relatively large CAPE that results in the increase of precipitation. They also pointed out that rainfall is usually in negative feedback with the SM at the onset stage of convection that is just triggered and initiated. Such negative feedback is less obvious in the two cases of our study, which is at least not strong enough to lead to change of the convection occurrence. Whether this is one of the specific

characteristics in South China, it needs to be confirmed by more case studies.

5 DISCUSSION

Applying WRF and its coupled Noah LSM, this work studies the effect of SM on heavy rainfall and mesoscale convective systems in South China. Two cases of heavy rain were selected: the first one is a localized late afternoon severe rain event and the second one occurred within a frontal low trough under an environment controlled by a more distinct large scale system.

The results from this study show some difference from those found in studies on the so-called "hot spots" where soil moisture has strong effect on rainfall. Does it have something to do with the following fact that South China is located in a low-latitude region that is adjacent to the ocean and subject to the southwesterly airflow and monsoon from the South China Sea? Usually with abundant water vapor, the atmosphere in this region is such that it is hard for the variation of land surface water and heat flux induced by the SM to play a decisive role in the convection development and rainfall occurrence. It will help to understand more about this issue if more case simulation studies are carried out and more factors associated with the land-surface processes are analyzed comprehensively.

REFERENCES:

[1] VITERBO P. Initial values of soil water and the quality of the summer forecasts [J]. ECMWF Newsletter, 1995, 69: 2-8.

[2] BELJAARS A C M, VITERBO P, MILLER M J, et al. The anomalous rainfall over the United States during July 1993: sensitivity to land surface parameterization and soil moisture anomalies [J]. Mon Wea Rev, 1996, 124 (3): 362-383.

[3] TAYLOR C M. Intraseasonal land-atmosphere coupling in the West African monsoon [J]. J Climate, 2008, 21(24): 6 636-6 648.

[4] KOSTER R D, DIRMEYER P A, GUO Z, et al. Regions of strong coupling between soil moisture and precipitation [J]. Science, 2004, 305(5 687): 1138-1140.

[5] MOHR K I, BAKER R D, TAO W K, et al. The sensitivity of West African convective line water budgets to land cover [J]. J Hydrometeorol, 2003, 4(1): 62-76.

[6] SOGALLA M, KRUGER A, KERSCHGENS M. Mesoscale modeling of interactions between rainfall and the land surface in West Africa [J]. Meteorol Atmos Phys, 2006, 91(1-4): 211-221.

[7] ALONGE C J, MOHR K I, TAO W K. Numerical studies of wet versus dry soil regimes in the West African Sahel [J]. J Hydrometeorol, 2007, 8(1): 102-116.

[8] TAYLOR C M, ELLIS R J. Satellite detection of soil moisture impacts on convection at the mesoscale [J]. Geophys Res Lett, 2006, 33, L03404, DOI:10.1029/2005GL025252.

[9] ZIEGLER C L, MARTIN W J, PIELKE R A, et al. A modeling study of a dryline [J]. J Atmos Sci, 1995, 52(2): 263-285.

[10] SHAW B L, PIELKE R A, ZIEGLER C L. A three-dimensional numerical simulation of a Great Plains dryline [J]. Mon Wea Rev, 1997, 125(7): 1489-1506.

[11] TRIER S B, CHEN F, MANNING K W. A study of convection initiation in a mesoscale model using high-resolution land surface initial conditions [J]. Mon Wea Rev, 2004, 132(12): 2954-2976.

[12] HOLT T R, NIYOGI D, CHEN F, et al. Effect of land-atmosphere interactions on the IHOP 24-25 May 2002 convection case [J]. Mon Wea Rev, 2006, 134(1): 113-133.

[13] MULLEN S L, BAUMHEFNER D P. Monte Carlo simulations of explosive cyclogenesis [J]. Mon Wea Rev, 1994, 122(7): 1548-1567.

[14] MARTIN W J, XUE M. Sensitivity analysis of convection of the 24 May 2002 IHOP case using very large ensembles [J]. Mon Wea Rev, 2006, 134(1): 192-207.

[15] CHEN F, DUDHIA J. Coupling an advanced land-surface/hydrology model with the Penn State/NCAR MM5 modeling system Part I: Model implementation and sensitivity [J]. Mon Wea Rev, 2001, 129(4): 569-585.

[16] CHEN F. The role of land-atmospheric interactions in the initiation of deep convection for convection- resolving regional-scale models[C]// American Geophysical Union, Fall Meeting 2007. http://adsabs.harvard.edu/abs/2007AGUSM.A51E..02C.

[17] LI Yu-lan, WANG Jing-rong, ZHENG Xin-jiang, et al. On the mesoscale convective complex in the southwest-south part of China [J]. Acta Atmos Sinica, 1989, 13(4): 417-422.

[18] ZHOU Xiu-ji. Experiments on Heavy Rains across the Taiwan Strait and Neighboring Areas [M]. Beijing: China Meteorological Press, 2000, 370.

[19] MENG Wei-guang, ZHANG Yan-xia, DAI Guang-feng, et al. The formation and development of a heavy rainfall mesoscale convective system along southern China coastal area [J]. J Trop Meteorol, 2007, 23(6): 521-530.

[20] ZHANG Xiao-mei, MENG Wei-guang, ZHANG Yan-xia, et al. Analysis of mesoscale convective systems associated with a warm sector heavy rainfall event over South China [J]. J Trop Meteorol, 2009, 25(5): 551-560.

[21] SKAMAROCK W C, KLEMP J B, DUDHIA J, et al. A description of the advanced research WRF Version 3 [S]. NCAR Tech Note NCAR/TN-475+STR, 113.

[22] RODELL M, HOUSER P R, JAMBOR U, et al. The Global Land Data Assimilation System [J]. Bull Amer Meteorol Soc., 2004, 85(3): 381-394.

[23] HOLTON J R. An Introduction to Dynamic Meteorology [M]. San Diego, 1992: 511.

[24] GANTNER L, KALTHOFF N. Sensitivity of a modeled life cycle of a mesoscale convective system to soil conditions over West Africa [J]. Quart J Roy Meteorol Soc, 136(s1): 471-482.

Citation: MENG Wei-guang, ZHANG Yan-xia, LI Jiang-nan et al. Sensitivity of mesoscale convective systems and associated heavy rainfall to soil moisture over South China [J]. J Trop Meteorol, 2017, 23(1): 91-102.